Acta Crystallographica Section F
Structural Biology and Crystallization Communications
ISSN 1744-3091

High crystallizability under air-exclusion conditions of the full-length LysR-type transcriptional regulator TsaR from *Comamonas testosteroni* T-2 and data-set analysis for a MIRAS structure-solution approach

Dominique Monferrer,[a] Tewes Tralau,[b] Michael A. Kertesz,[c] Santosh Panjikar[d] and Isabel Usón[e]*

[a]IBMB–CSIC, Baldiri Reixach 15, 08028 Barcelona, Spain, [b]University of Manchester, Faculty of Life Sciences, Manchester Interdisciplinary Biocentre, 131 Princess Street, Manchester M1 7DN, England, [c]University of Manchester, Faculty of Life Sciences, Michael Smith Building D1413, Manchester M13 9PT, England, [d]EMBL Hamburg Outstation, c/o DESY, Notkestrasse 85, D-22603 Hamburg, Germany, and [e]ICREA at IBMB-CSIC, Baldiri Reixach 15, 08028 Barcelona, Spain

Correspondence e-mail: uson@ibmb.csic.es

Received 6 May 2008
Accepted 27 June 2008

The full-length LysR-type transcriptional regulator TsaR from *Comamonas testosteroni* T-2 was heterologously overexpressed in *Escherichia coli*, purified and stabilized under conditions that favoured its rapid crystallization using the microbatch-under-oil technique. The purified protein was highly crystallizable and two different crystal forms were readily obtained. However, only monoclinic crystals gave diffraction beyond 2 Å and there was a slight variation in unit-cell parameters between crystals. The only other LysR-type regulator for which a full-length crystal form is available is CbnR, but no solution could be obtained when this was used as a model in molecular replacement. Mercury and xenon derivatives were therefore produced in order to phase the structure using a MIRAS approach.

1. Introduction

TsaR is a 298-amino-acid protein that belongs to the LysR family of transcriptional regulators (LTTR) and controls the expression of the operon *tsaMBCD* in the soil bacterium *Comamonas testosteroni* T-2. The *tsaMBCD* genes encode the enzymes required for the initial desulfonation of *p*-toluenesulfonate, an industrial arylsulfonate and major pollutant (Tralau *et al.*, 2003). The initial desulfonation leads to the formation of protocatechuate and is followed by oxidative ring cleavage, thus allowing the organism to use *p*-toluenesulfonate as a sole source of carbon and energy (Cook *et al.*, 1999). This use of an arylsulfonate as a carbon source contrasts with the alternative use of arylsulfonates as a sulfur source by many other organisms, which is upregulated under sulfate-limitation conditions (Kertesz, 2000). The degradation of compounds as carbon and energy sources tends to be regulated on the operon and gene level by individual regulators, while transcriptional control under sulfate limitation is a coordinated response of the CysB regulon and individual regulators (Van der Ploeg *et al.*, 1996). Characterization of the regulators for these degradative pathways has merited attention owing to their biotechnological relevance for the bioremediation of polluted waste waters and effluents from waste dumps.

LTTRs are the most common regulators in prokaryotes and have been the subject of intense study ever since the term LTTR was first introduced (Henikoff *et al.*, 1988). They are characterized by two main domains: an N-terminal domain with a winged helix–turn–helix (wHTH) as a DNA-binding motif and a helix 30 residues in length and a C-terminal region made up of two subdomains with α/β Rossmann-fold topology. The full-length proteins are homotetrameric in solution and their ability to bind to multiple sites within a promoter region is mediated by the presence of a small coinducer, which is often a metabolite of the pathway they regulate (Schell, 1993). Very few LTTR crystal structures have been obtained. This is partly because of their general low solubility but presumably also because of their inherent flexibility; they are composed of two distinct domains joined by a flexible linker. Indeed, all but one of the LTTR structures available have been determined using truncated forms of the respective proteins and show only the C-terminal domain, as for BenM (Ezezika *et al.*, 2007) and DntR (Smirnova *et al.*, 2004) among other cases. The structure of CbnR is the only full-length crystal

structure of a LysR regulator that has been determined to date (Muraoka *et al.*, 2003).

Here, we report that full-length TsaR displays high crystallizability when it is purified and crystallized under conditions that stabilize the protein in solution and allow the exclusion of air. We describe the efforts made to resolve several problems that were encountered during the process of crystallographic phasing, namely non-isomorphism, as previously reported in the case of CysB phasing (Verschueren *et al.*, 1999), low substitution of heavy atoms and incompleteness and anisotropy as a consequence of the low-symmetry space group.

2. Materials and methods

2.1. Protein expression and purification

C-terminally His-tagged TsaR was heterologously overexpressed in *Escherichia coli* M10 (Tralau *et al.*, 2003). Cells were grown semi-aerobically in LB medium (1 l medium in 2 l Erlenmeyer flasks) in the presence of kanamycin (25 µg ml^{-1}) and ampicillin (100 µg ml^{-1}) at 303 K and 180 rev min^{-1}. Overexpression was induced by the addition of 1 m*M* IPTG at an OD_{600} of 0.4. Cells were harvested by centrifugation (30 000*g*, 277 K, 30 min) 2 h after induction, washed in 50 m*M* Tris–HCl pH 8.0 and stored at 253 K until further processing. The pellet obtained from 2 l cell culture was resuspended in 40 ml lysis buffer (20 m*M* Tris–HCl pH 7.0, 0.3 *M* NaCl) containing either 200 µ*M* PMSF or a tablet of complete EDTA-free protease-inhibitor cocktail (Roche) and 10 ng ml^{-1} DNAse I. Cells were lysed using a Cell Disruptor (Constant Systems Ltd) applying a pressure of 1.35 MPa and centrifuged for 30 min at 40 000*g*.

For Ni-affinity purification of the TsaR protein, the amount of TsaR in the crude lysate was estimated by SDS–PAGE and the quantity of Ni–NTA Superflow resin (Qiagen) calculated to be required to bind half of the total TsaR present was then added. After a short incubation, unbound proteins were removed by three successive washing steps using lysis buffer containing increasing concentrations of imidazole (20, 40 and 80 m*M*) and TsaR was then eluted with 0.3 *M* imidazole in lysis buffer supplemented with 1 *M* β-mercaptoethanol as in the original literature (Tralau *et al.*, 2003). The purified protein was concentrated as required using Centricon YM-10 and Microcon YM-10 concentrators (Amicon, Millipore).

In subsequent preparations, the protocol was optimized in order to avoid interference from β-mercaptoethanol. Ni-affinity chromatography was preceded by the removal of excess nucleic acids from the centrifuged lysate by incubation with 0.15% polyethyleneimine (PEI) pH 7.0 at 277 K for 10 min. Precipitated material was removed by centrifugation at 40 000*g* for 30 min and the clarified supernatant was then filtered through a 0.22 µm membrane (Millex, Millipore) and immediately purified as described above. This procedure dramatically improved the quantity and quality of the purified protein. When this procedure was used, the salt content of all buffers was increased to 0.5 *M* NaCl to maintain the solubility of the protein and 5%(*v*/*v*) glycerol and 5 m*M* tris(2-carboxyethyl)phosphine (TCEP) were added to the elution buffer. Owing to the viscosity of the glycerol and the use of an alternative reducing agent, the corresponding protein preparations did not require the addition of β-mercaptoethanol.

Gel-filtration chromatography (Superdex-200, Pharmacia) showed that TsaR eluted as a tetramer when purified under the above conditions.

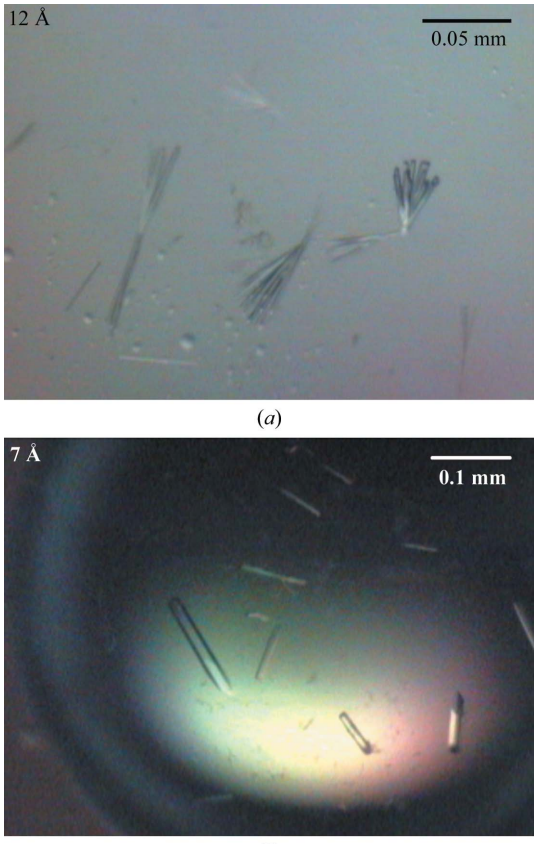

Figure 1
(*a*) Initial crystals of TsaR obtained by hanging-drop vapour diffusion in 1 *M* glycine pH 8.0 and 0.5 *M* NaCl. (*b*) Optimization of the same conditions by the addition of 0.1 *M* NaI.

2.2. Crystallization and preliminary crystal assessment

The first crystals of TsaR were obtained from a sample stored at 253 K in 20% glycerol during a buffer screening aimed at determining suitable conditions for dialysis of the protein prior to attempting crystallization. A 2 mg ml^{-1} protein solution mixed with 1 *M* glycine pH 8, 0.5 *M* NaCl in a 1:1 ratio yielded needle-like crystals after overnight equilibration at 293 K using the hanging-drop vapour-diffusion method. These crystals had dimensions of 0.15 × 0.05 × 0.05 mm and diffracted to 12 Å resolution using the in-house X-ray facilities (single rotation-axis diffractometer with a MAR 345 image-plate detector mounted on a rotating-anode X-ray generator (Cu $K\alpha$, λ = 1.5418 Å; Fig. 1*a*). The addition of 100 m*M* NaI to the crystallization solution improved the quality of the crystals remarkably; they diffracted to 7 Å resolution at the synchrotron (ID14-EH2, ESRF; Fig. 1*b*).

Fresh protein was prepared as described above in order to improve the diffraction quality of the crystals and drops containing 1 µl 5 mg ml^{-1} TsaR solution and 1 µl reservoir solution were set up with Crystal Screen I (CSI; Hampton Research) at 277 and 293 K using the microbatch-under-oil technique. More than 20% of the 50 conditions of the screen produced 'hits' at 293 K in a few days; these ranged from crystalline precipitate to visible crystals. A plate-like monoclinic crystal form appeared in two conditions based on 0.1 *M* sodium acetate pH 4.6: condition No. 20 [0.2 *M* $(NH_4)_2SO_4$, 25%(*w*/*v*) PEG 4000; Fig. 2*c*] and condition No. 34 (2 *M* sodium formate; Fig. 2*a*). In both conditions the crystals appeared overnight and reached final dimensions within 3 d. These crystals diffracted to 2.5 Å resolution at the in-house facility (Fig. 3*a*).

A second crystal form, showing a tetragonal lysozyme-like habit, appeared in condition No. 11 [1 *M* $NH_4H_2PO_4$, 0.1 *M* trisodium citrate pH 5.6) and condition No. 48 (2 *M* $NH_4H_2PO_4$, 0.1 *M* Tris–HCl pH 8.5; Fig. 2*d*), but failed to diffract beyond 7 Å resolution using a synchrotron source (Fig. 3*b*). At this stage, condition No. 34 was selected because of the larger size and better reproducibility of the crystals and the second crystal form was not further optimized.

Crystals from condition No. 34 were also grown in capillaries of 0.2 and 0.3 mm diameter prepared by mixing the protein sample in a 1:1 ratio with low-melting-temperature agarose at 0.2%(*w*/*v*) in the same elution buffer. In some cases a 0.5%(*w*/*v*) agarose plug was placed between the crystallization-condition and the protein chambers (Fig. 2*b*). This capillary-based counter-diffusion batch technique (García-Ruiz, 2003) produced crystals of good diffraction quality and

Table 1
Data-collection statistics for native crystals.

Values in parentheses are for the highest resolution shells.

Data sets	Native 1	Native 2	Native 3	Native 4	Native 5	Native 6	Native 7
Source	ID14-EH2	In-house†	In-house	ID14-EH2	In-house	BM16	ID14-EH2
Wavelength (Å)	0.9326	1.5418	1.5418	0.9326	1.5418	1.6059	0.9326
Space group	*C*2	*C*2	*C*2	*C*2	*C*2	*C*2	$P4_12_12$ or $P4_32_12$
Unit-cell parameters (Å, °)	*a* = 135.74, *b* = 51.39, *c* = 108.44, *β* = 110.94	*a* = 136.80, *b* = 51.88, *c* = 109.39, *β* = 111.52	*a* = 135.02, *b* = 51.49, *c* = 108.47, *β* = 110.55	*a* = 134.70, *b* = 51.74, *c* = 108.03, *β* = 110.81	*a* = 135.35, *b* = 51.77, *c* = 109.08, *β* = 111.11	*a* = 136.49, *b* = 51.48, *c* = 107.75, *β* = 110.35	*a* = 204.37, *b* = 204.37, *c* = 336.21
Resolution (Å)	19.61–1.80 (1.89–180)	49.59–2.67 (2.77–2.67)	47.15–1.79 (1.89–1.79)	48.74–2.11 (2.21–2.11)	47.90–2.01 (2.10–2.01)	32.85–2.51 (2.59–2.51)	49.57–7.10 (7.20–7.10)
Unique reflections	52705 (7371)	20391 (1891)	64424 (8299)	39480 (4244)	43670 (4140)	24352 (2422)	11299 (449)
Redundancy	3.75 (3.76)	3.46 (2.55)	7.03 (5.68)	1.89 (1.60)	5.65 (1.61)	3.87 (3.83)	7.71 (8.14)
Completeness (%)	99.3 (99.1)	98.7 (88.5)	96.6 (81.9)	98.2 (86.0)	95.9 (72.0)	99.9 (100)	99.3 (100)
R_{merge}‡ (%)	4.21 (51.32)	4.24 (13.9)	2.98 (18.2)	4.18 (27.8)	5.93 (49.5)	2.99 (13.92)	4.75 (36.03)
R_{int} (%)	5.53 (57.73)	4.81 (13.03)	5.76 (34.20)	5.79 (20.22)	9.53 (30.49)	3.77 (17.71)	10.58 (60.87)
$I/\sigma(I)$	15.90 (2.14)	16.97 (7.09)	24.62 (5.72)	16.50 (4.13)	11.35 (2.32)	23.49 (7.04)	17.70 (2.95)

† In-house X-ray facilities were a single rotation-axis diffractometer with a MAR 345 image-plate detector mounted on a rotating-anode X-ray generator. ‡ $R_{merge} = \sum_{hkl}\sum_i |I_i(hkl) - \langle I(hkl)\rangle| / \sum_{hkl}\sum_i I_i(hkl)$.

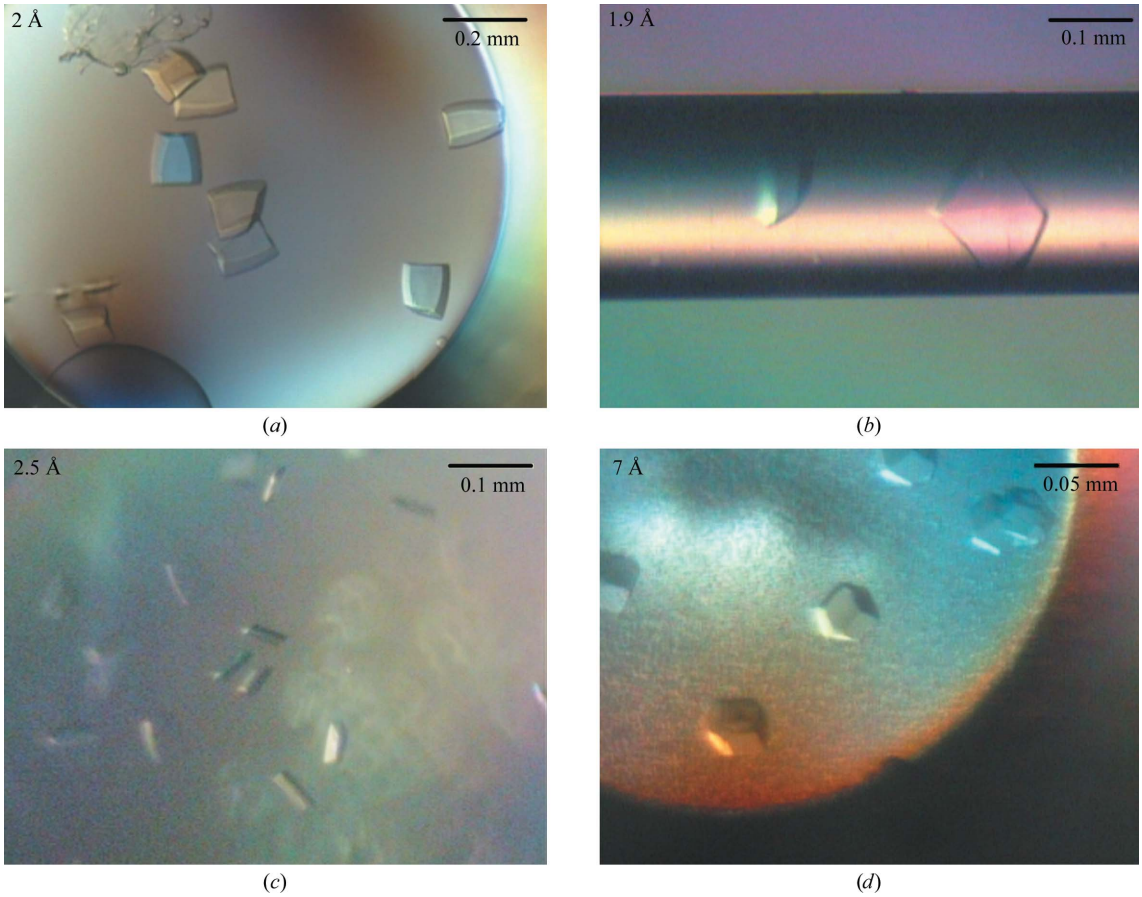

Figure 2
Crystals obtained using the microbatch-under-oil technique at 293 K with condition No. 34 of Crystal Screen I (CSI; Hampton Research). (*b*) The same condition in a 0.2 mm internal diameter capillary. (*c*) and (*d*) Crystals obtained using the microbatch-under-oil technique at 293 K with (*c*) condition No. 20 and (*d*) condition No. 48 of CSI.

facilitated transport to other laboratories, where experiments that required *in situ* crystal manipulation prior to data collection were successfully performed.

Crystals were cryoprotected with solutions prepared for each CSI condition according to the specified relative crystallization conditions of Crystal Screen Cryo (Hampton Research) for data collection at 100 K (Garman & Schneider, 1997): 0.16 *M* $(NH_4)_2SO_4$, 0.08 *M* sodium acetate pH 4.6, 20%(*w*/*v*) PEG 4000 and 20%(*v*/*v*) anhydrous glycerol for condition No. 20, 0.07 *M* sodium acetate pH 4.6, 1.4 *M* sodium formate and 30%(*v*/*v*) anhydrous glycerol for condition No. 34 and 0.08 *M* Tris–HCl pH 8.5, 1.6 *M* $NH_4H_2PO_4$ and 20%(*v*/*v*) anhydrous glycerol for condition No. 48.

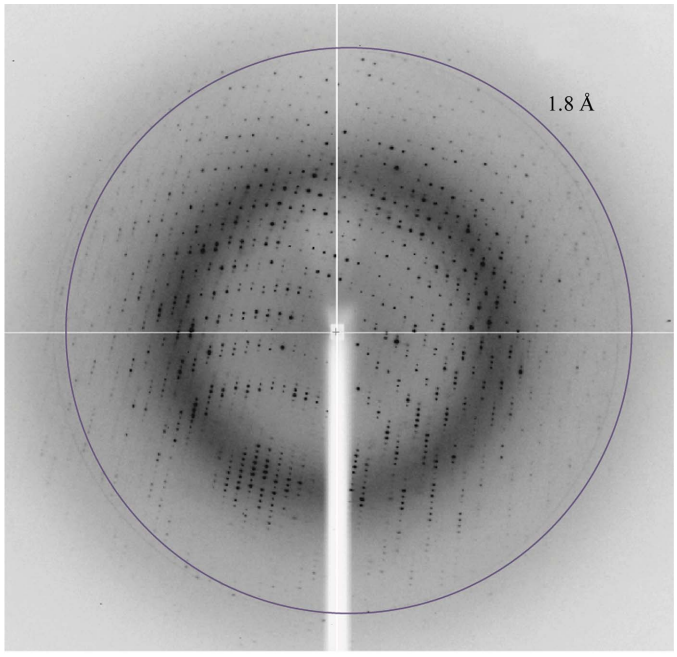

(*a*)

(*b*)

Figure 3
Diffraction patterns of (*a*) *C*2 crystals grown using condition No. 34 of CSI and (*b*) $P4_12_12$ or $P4_32_12$ crystals grown using condition No. 48 of CSI.

2.3. Data collection and processing

Native and derivative data sets were collected using in-house and synchrotron X-ray sources from crystals grown in condition No. 34 (Table 1). Native 1 had many reflections missing in the low-resolution range and a composite data set was therefore prepared with Natives 1 and 2 in order to complement the missing reflections. However, this could not be used for phasing because the resultant data set was not isomorphous with the derivatives (data not shown). Native 3 was collected after a quick soak of a crystal in 1 *M* NaCl in an attempt to create a more isomorphous data set relative to several halide-derivatization trials performed with crystals grown in 0.1 *M* NaI (Native 4) or quick-soaked in 1 *M* NaI (Native 5). Native 6 was collected on a crystal that had been soaked in samarium(III) acetate without substitution of the heavy atom.

A data set from a crystal grown in condition No. 48 was collected using synchrotron radiation (Native 7, Table 1). In spite of the low resolution, it was possible to determine that it belonged to either space group $P4_12_12$ or $P4_32_12$, with unit-cell parameters $a = b = 204.37$, $c = 336.21$ Å. From the Matthews coefficient (Matthews, 1968) and the mechanical fragility of the crystals, the asymmetric unit is likely to contain three or four tetramers (Matthews coefficient of 3.32 $Å^3$ Da^{-1} and 63% solvent content with 16 molecules or 72% for 12 molecules in the asymmetric unit). A different asymmetric unit content cannot be excluded although it appears to be less likely. A self-rotation function was calculated as a means of supporting one or the other possibility and two clear peaks of equal intensity at 90% height from the origin peak were found at $\omega = 90$, $\varphi = 31^\circ$ and $\omega = 90$, $\varphi = 14^\circ$ and their equivalents. These corresponded to two independent noncrystallographic symmetry axes that could relate two pairs of tetramers in the asymmetric unit (Fig. 4).

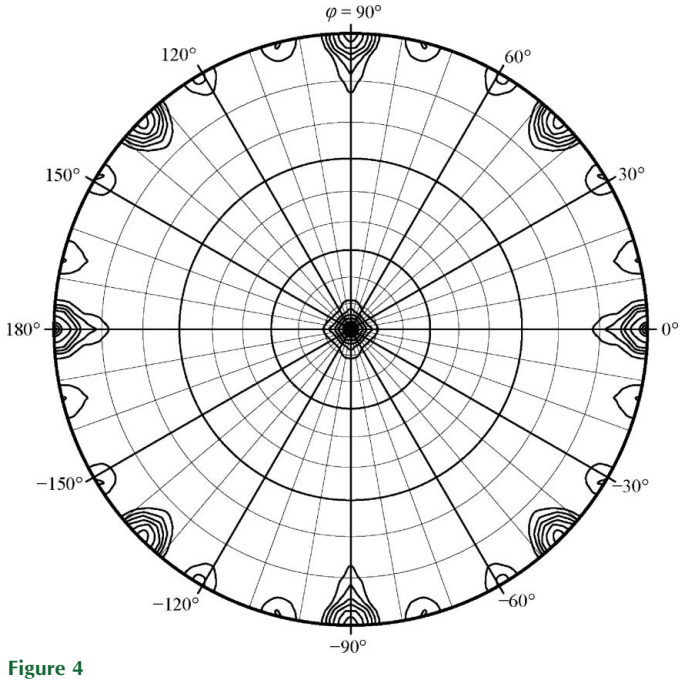

Figure 4
Stereographic projection for a data set collected from a crystal grown using condition No. 48 of CSI ($P4_12_12$ or $P4_32_12$); the $\kappa = 180^\circ$ section shows two peaks of equal height (90% of the origin peak) at polar angles $\omega = 90$, $\varphi = 31^\circ$ and $\omega = 90$, $\varphi = 14^\circ$. This figure was prepared using *XPREP* (Sheldrick, 1997).

Table 2
Data-collection statistics for derivative crystals.

Values in parentheses are for the highest resolution shells.

	Hg1				
Data sets	Peak	Inflection point	Remote	Hg2	Xe
Source	ID29			In-house†	BW7A
Wavelength (Å)	1.0075	1.0088	1.0052	1.5418	0.9763
Space group	*C*2			*C*2	*C*2
Unit-cell parameters (Å, °)	a = 134.70, b = 51.74, c = 108.03, β = 110.80			a = 136.52, b = 51.49, c = 107.74, β = 110.35	a = 136.52, b = 51.49, c = 107.74, β = 110.36
Resolution (Å)	19.99–2.40 (2.49–2.40)	19.99–2.40 (2.49–2.40)	19.99–2.40 (2.49–2.40)	19.68–2.63 (2.72–2.63)	20.06–2.47 (2.57–2.47)
Unique reflections	26427 (2746)	26400 (2721)	46852 (4652)	21267 (2041)	24743 (2088)
Redundancy	1.70 (1.68)	1.70 (1.68)	1.70 (1.68)	1.84 (1.82)	1.86 (1.38)
Completeness (%)	95.9 (97.0)	95.9 (96.8)	95.9 (97.0)	99.7 (100)	96.5 (71.5)
$R_{\rm merge}$‡ (%)	7.22 (46.4)	7.23 (43.72)	7.20 (46.96)	12.70 (43.52)	2.43 (19.04)
$R_{\rm int}$ (%)	7.04 (36.48)	6.61 (35.33)	6.79 (36.18)	10.68 (22.79)	2.38 (12.90)
$I/\sigma(I)$	10.30 (2.36)	10.28 (2.49)	10.35 (2.33)	8.38 (2.53)	30.98 (5.59)

† In-house X-ray facilities were a single rotation-axis diffractometer with a MAR 345 image-plate detector mounted on a rotating-anode X-ray generator. ‡ $R_{\rm merge} = \sum_{hkl}\sum_i |I_i(hkl) - \langle I(hkl)\rangle|/\sum_{hkl}\sum_i I_i(hkl)$.

Derivatives were prepared from native crystals grown in condition No. 34. Two Hg derivatives were obtained by soaking the crystals in 10 m*M* thimerosal overnight and a xenon derivative was obtained by pressurizing crystals of TsaR grown in capillaries (Schiltz *et al.*, 2003). For xenon derivatization, the crystal was transferred to a cryoprotectant and was then picked up in a cryoloop. The cryoloop was then placed inside a xenon pressure cell from Hampton Research (EMBL Hamburg Outstation, Germany) in which a vial of the cryoprotectant had been previously placed to prevent the crystal drying out. The cell was pressurized to 2 MPa xenon for 1 min at 293 K. After releasing the pressure over 10–15 s, the sample was immediately flash-cooled in liquid nitrogen.

Data sets were processed with *XDS* (Kabsch, 1988) or *HKL*-2000 (Otwinowski & Minor, 1997) and analysed with *XPREP* (Sheldrick, 1997).

2.4. Heavy-atom substructure solution for MIRAS

The problems encountered in phasing the structure of TsaR were largely the consequence of a small but general lack of isomorphism among the several data sets collected, incompleteness of the low-resolution range for most of the data sets and for the MAD data set because of the mounting of the monoclinic crystals along the unique axis and low substitution of the heavy atoms in each of the derivatives, with a consequent weak anomalous signal.

Attempts to phase TsaR by molecular replacement using the separate domains of CbnR as search model were unsuccessful.

As the protein contains four cysteine residues, which are presumably not involved in disulfide bridges, heavy-atom derivatization was chosen rather than the production of a selenomethionine derivative. A Hg-MAD data set was collected (Hg1, Table 1), but the incompleteness of the anomalous data required the collection of an in-house data set (Hg2, Table 1) to combine into a composite Hg data set (data not shown).

3. Results and discussion

High concentrations of viscous components such as imidazole and glycerol have proven to be necessary to keep LTTRs in solution in previous studies (Verschueren *et al.*, 1999; Stec *et al.*, 2004). In the case of TsaR, the oxygen-sensitivity of the protein posed additional problems and high concentrations of β-mercaptoethanol (1 *M*) were initially used to keep it stable (Tralau *et al.*, 2003). It was not possible to dialyse the purified protein into buffers that would be more suitable for testing a wide range of crystallization conditions, although the addition of 5% glycerol was effective in reducing the concentration of β-mercaptoethanol to 50 m*M* or substituting it by 5 m*M* TCEP. In addition to the presence of the reducing agent, the exclusion of air was required throughout TsaR preparation and crystallization, with semi-aerobic culture parameters used in the overexpression step (limited oxygenation of the growth medium was achieved by 50% filling of nonbaffled flasks and slow agitation) and stabilization of the purified protein in viscous buffers. Crystallization was carried out in batches with limited or no oxygen diffusion. Indeed, the only techniques that led to diffraction-quality crystals were the microbatch-under-oil method with 50% silicon and 50% paraffin oil (Al's Oil, Hampton Research) and the use of sealed capillaries.

The batch-capillary technique was used as a means of optimizing crystallization in condition No. 34 of CSI by further screening the effect of counter-diffusion. Crystals grew to similar or even larger sizes than those obtained using the microbatch-under-oil technique, with the additional advantage that transport of the crystals to other laboratories or light sources was greatly facilitated.

The high crystallizability shown by TsaR, with crystalline material being obtained in 20% of the CSI conditions at 293 K, was a consequence of the fragile equilibrium attained by adding high concentrations of potential precipitants to the stabilization buffer (organic solvents and salt). In this case the effectiveness of the buffering capacity in any given crystallization condition was unclear, since the imidazole concentration in the protein solution was three times the concentration of the stabilization buffer. Surprisingly, however, only crystallization conditions with moderately low pH yielded reproducible crystals. In particular, of the 10% of hits with visible crystals, only four were reproducible. It is possible that conditions based on lower salt concentrations and on volatile organic solvents such as 2-propanol were more sensitive to the final imidazole concentration in the drop and therefore unable to displace the pH of the buffered TsaR to lower values. It is interesting to note that the TsaR crystallization conditions resemble those described for the C-terminal domains of two LTTRs: BenM and CatM. In this case, condition No. 20 of the CSI set up using microbatch-under-oil crystallization was reported to lead to the formation of orthorhombic crystals (Clark *et al.*, 2004).

Crystallization conditions Nos. 11, 20, 34 and 48 share two common characteristics: the presence of high concentrations of salt as preci-

pitant [2 *M* sodium formate and $NH_4H_2PO_4$ in conditions Nos. 34 and 48, respectively, 1 *M* $NH_4H_2PO_4$ in condition No. 11 and 0.2 *M* $(NH_4)_2SO_4$ in condition No. 20] and a slightly acidic pH between 5 and 6. Despite the sodium acetate buffer at pH 4.6 in conditions Nos. 20 and 34, the final pH values are 5 and 6, respectively. Sodium citrate buffers condition No. 11 at pH 5.6 and hydrolysis of the ammonium brings condition No. 48 into the same acid range, despite the presence of 0.1 *M* Tris–HCl pH 8.5.

The salts $NH_4H_2PO_4$ and $(NH_4)_2SO_4$ should be able to form similar crystal contacts, but they presumably lead to different crystal forms. Solving the structure of this second crystal form could possibly reveal patches of positively charged residues that coordinate the PO_4^{3-} present in the crystallization condition, thus mimicking the DNA–phosphate backbone that interacts with the residues of the DNA-binding sites. More interestingly, the fact that the analogous SO_4^{2-}-containing salt does not lead the molecules to crystallize in the same space group suggests a competing effect of the sulfate ligand with phosphate recognition. This seems to be in accordance with the modulatory DNA-binding effect observed with TsaR and *p*-toluenesulfonate as co-inducer (Tralau *et al.*, 2003).

The substructures of the two available derivatives were determined using *SHELXD* (Sheldrick, 2008). Three Hg positions and a Xe atom were found and placed with the same origin by cross-difference Fourier calculations on the phases obtained with the Hg composite derivative and refined with *SHELXE* (Sheldrick, 2008) until convergence was reached. MIRAS phasing and model building are currently in progress.

We are grateful to F. X. Gomis-Rüth and P. Fuentes-Prior for helpful discussion. This work was funded by grant BIO2006-14139 from the Spanish Ministerio de Educación y Ciencia and a fellowship of the IP3 Program of the Spanish Ministerio de Educación y Ciencia. Beamtime allocations at ESRF Grenoble and at the EMBL Outstation in Hamburg are gratefully acknowledged.

References

Clark, T., Haddad, S., Neidle, E. & Momany, C. (2004). *Acta Cryst.* D**60**, 105–108.
Cook, A. M., Laue, H. & Junker, F. (1999). *FEMS Microbiol. Rev.* **22**, 399–419.
Ezezika, O. C., Haddad, S., Clark, T. J., Neidle, E. L. & Momany, C. (2007). *J. Mol. Biol.* **367**, 616–629.
García-Ruiz, J. M. (2003). *Methods Enzymol.* **368**, 130–154.
Garman, E. F. & Schneider, T. R. (1997). *J. Appl. Cryst.* **30**, 211–237.
Henikoff, S., Haughn, G. W., Calvo, J. M. & Wallace, J. C. (1988). *Proc. Natl Acad. Sci. USA*, **85**, 6602–6606.
Kabsch, W. (1988). *J. Appl. Cryst.* **21**, 916–924.
Kertesz, M. A. (2000). *FEMS Microbiol. Rev.* **24**, 135–175.
Matthews, B. W. (1968). *J. Mol. Biol.* **33**, 491–497.
Muraoka, S., Okumura, R., Ogawa, N., Nonaka, T., Miyashita, K. & Senda, T. (2003). *J. Mol. Biol.* **328**, 555–566.
Otwinowski, Z. & Minor, W. (1997). *Methods Enzymol.* **276**, 307–326.
Ploeg, J. R. van der, Weiss, M. A., Saller, E., Nashimoto, H., Saito, N., Kertesz, M. A. & Leisinger, T. (1996). *J. Bacteriol.* **178**, 5438–5446.
Schell, M. A. (1993). *Annu. Rev. Microbiol.* **47**, 597–626.
Schiltz, M., Fourme, R. & Prangé, T. (2003). *Methods Enzymol.* **374**, 83–119.
Sheldrick, G. M. (1997). *XPREP*. Bruker AXS Inc., Madison, Wisconsin, USA.
Sheldrick, G. M. (2008). *Acta Cryst.* A**64**, 112–122.
Smirnova, I. A., Dian, C., Leonard, G. A., McSweeney, S., Birse, D. & Brzezinski, P. (2004). *J. Mol. Biol.* **340**, 405–418.
Stec, E., Witkowska, M., Hryniewicz, M. M., Brzozowski, A. M., Wilkinson, A. J. & Bujacz, G. D. (2004). *Acta Cryst.* D**60**, 1654–1657.
Tralau, T., Mampel, J., Cook, M. A. & Ruff, J. (2003). *Appl. Environ. Microbiol.* **69**, 2298–2305.
Verschueren, K. H. G., Tyrrell, R., Murshudov, G. N., Dodson, E. J. & Wilkinson, A. J. (1999). *Acta Cryst.* D**55**, 369–378.